

Research Article

Impact of climate changes on Arizona State precipitation patterns using high-resolution climatic gridded datasets

Hayder H. Kareem^{1*}, Shahla Abdulqader Nassrullah²

¹ Structures and Water Resources Engineering Department, Faculty of Engineering, University of Kufa, Al-Najaf, Iraq.

² Institute of Technology, Middle Technical University, Baghdad, Iraq.

Abstract: Climate change significantly affects environment, ecosystems, communities, and economies. These impacts often result in quick and gradual changes in water resources, environmental conditions, and weather patterns. A geographical study was conducted in Arizona State, USA, to examine monthly precipitation concentration rates over time. This analysis used a high-resolution 0.50×0.50 grid for monthly precipitation data from 1961 to 2022, Provided by the Climatic Research Unit. The study aimed to analyze climatic changes affected the first and last five years of each decade, as well as the entire decade, during the specified period. GIS was used to meet the objectives of this study. Arizona experienced 51–568 mm, 67–560 mm, 63–622 mm, and 52–590 mm of rainfall in the sixth, seventh, eighth, and ninth decades of the second millennium, respectively. Both the first and second five year periods of each decade showed acceptable rainfall amounts despite fluctuations. However, rainfall decreased in the first and second decades of the third millennium, and in the first two years of the third decade. Rainfall amounts dropped to 42–472 mm, 55–469 mm, and 74–498 mm, respectively, indicating a downward trend in precipitation. The central part of the state received the highest rainfall, while the eastern and western regions (spanning north to south) had significantly less. Over the decades of the third millennium, the average annual rainfall every five years was relatively low, showing a declining trend due to severe climate changes, generally ranging between 35 mm and 498 mm. The central regions consistently received more rainfall than the eastern and western outskirts. Arizona is currently experiencing a decrease in rainfall due to climate change, a situation that could deteriorate further. This highlights the need to optimize the use of existing rainfall and explore alternative water sources.

Keywords: Spatial Analysis; Climate Impact; Precipitation Rates; CRU Dataset; GIS; Arizona State; USA

Received: 15 Jun 2024/ Accepted: 29 Sep 2024/ Published: 20 Feb 2025

Introduction

The concentration of precipitation is a key factor when characterizing the climate of a particular area or region, as it supplements traditional variables like annual precipitation and seasonality. Precipita-

tion concentration also helps in assessing risks associated with extreme precipitation events (Senviratne and Neville, 2012; Donat et al. 2013). To effectively analyze and characterize regional-scale precipitation patterns, it is essential to use data with both high temporal and spatial resolution. This level of precision is necessary due to the rapid changes in precipitation over time and space.

The significance of high-quality, gridded datasets has been highlighted by several researchers, including Trenberth (1997) and Goddard et al. (2001), who emphasized the growing importance of these datasets in climate research. Gridded datasets, which undergo strict quality control and provide historical climate data, are particularly valuable. In recent years, there has been a growing

*Corresponding author: Hayder H. Kareem, E-mail address: hayderh.alshaibani@uokufa.edu.iq

DOI: 10.26599/JGSE.2025.9280037

Kareem Hayder H, Nassrullah SA. 2025. Impact of climate changes on Arizona State precipitation patterns using high-resolution climatic gridded datasets. Journal of Groundwater Science and Engineering, 13(1): 34-46.

2305-7068/© 2025 Journal of Groundwater Science and Engineering Editorial Office This is an open access article under the CC BY-NC-ND license (<http://creativecommons.org/licenses/by-nc-nd/4.0>)

demand for comprehensive, frequently updated gridded datasets that provide high-resolution information, both temporally and spatially. Such datasets have wide applications in various fields, including hydrology, agriculture, and healthcare.

Osborn and Hulme (1997) illustrated the vital role of gridded data in evaluating and validating global and regional climate models. Furthermore, statistical downscaling strategies, as described by Maurer and Hidalgo (2008), are critical for adapting global climate predictions to more localized, regional contexts.

However, as human activities continue to emit greenhouse gases into the atmosphere, climate change is causing significant shifts in precipitation patterns. Numerous scientific studies have explored the complex relationship between climate change and these evolving precipitation patterns. The Intergovernmental Panel on Climate Change (IPCC), a leading international body, has released assessment reports detailing both projected rainfall scenarios and real-time observations of changes in precipitation levels. The IPCC's Fifth Assessment Report (2014) and Sixth Assessment Report (2021) provide comprehensive insights into rainfall trends, emphasizing the understanding of the hydrological cycle and dynamic atmospheric changes.

Rising global temperatures, driven by the phenomenon of global warming, intensify evaporation from Earth's water bodies, leading to increased atmospheric humidity. This can result in more frequent and intense rain events in some regions, while in others, precipitation may decline. The increased frequency and intensity of heavy rainfall and flooding disasters worldwide are evidence of this shift. In contrast, alterations in atmospheric circulation patterns driven by climate change can lead to reduced precipitation in certain areas (Cai et al. 2014).

The impact of these changes varies across different regions, as local factors interact with broader global climate patterns. For instance, the Arctic and other high-latitude regions are warming rapidly, causing a shift from snow to rain in precipitation, which disrupts local ecosystems and affects the livelihoods of indigenous communities (Groisman et al. 2005).

The spatial and temporal evaluation of rainfall patterns is a critical area of research, as it offers valuable insights into the complex processes of climate variability and adaptation. Recent advancements in environment modeling have enabled scientists to simulate and project future rainfall patterns under diverse climate change scenarios (Trenberth et al. 2003). To perform comprehen-

sive regional and local evaluations, datasets with significantly enhanced spatial and temporal resolutions are essential, often requiring a scale of tens of kilometers in space combined with intra-day or daily time granularity. This level of detail is necessary to differentiate atmospheric changes among sub-regions and to conduct a comprehensive analysis of both standard and extreme climate conditions.

In recent years, there have been significant advances in the development of daily gridded datasets that cover entire continents. These datasets are created by integrating large networks of daily rainfall data collected from numerous monitoring stations. Such datasets have been generated for various regions, including Europe, as shown by Haylock et al. (2008), North America, as highlighted by Maurer and Hidalgo (2008), South America, as reviewed by Liebmann and Allured (2005), and Asia, as detailed by Yatagai et al. (2009). These datasets generally offer resolutions of approximately 50 kilometers, allowing for analyses of ordinary environment problems across large inland areas.

High-resolution satellite data were utilized in a study by Mishra et al. (2022) to examine the geographical distribution of rains across India, aiming to identify local patterns and trends in precipitation over recent years. Behrangi et al. (2021) focused on a global rainfall analysis using satellite-based data, leveraging advancements in remote sensing technology to investigate temporal and spatial variations in precipitation on a worldwide scale. Environment models also play a crucial role in comprehending rains patterns. Shekhar et al. (2020) performed examinations on rainfall to reveal severe temporal and geographic variations in areas of South Asia by developing models that simulate weather conditions. The Global Precipitation Measurement (GPM) project, as detailed by Huffman et al. (2017) is a national initiative providing continuous and highly reliable rainfall data for global climate research, relying on satellite information. Zhang et al. (2019) conducted a long-term study in China examining extreme variations in rainfall based on scale analyses and satellite data. Swain and coworkers (2022) focused on local and temporal patterns of rainfall variability in the Himalayan region. Zhang et al. (2021) performed a comprehensive global assessment of long-term changes in rainfall, with particular emphasis on the impact of human-induced environmental change. Additionally, Song et al. (2021) explored the effect of urbanization on spatial rainfall patterns within urbane contexts.

Meteorological spatial data that aligns with observational data is essential across several scientific fields, including environmental, hydrology, agriculture, renewable energy applications, biology, economy, and sociology (Sun et al. 2018). Among various weather variables, precipitation is the key driver of the hydrological cycle and is often the most challenging element to estimate. Precipitation datasets are critical for informing hydrological models, such as the Soil & Water Assessment Tool (SWAT), Geographic Information System (GIS), and the Topography Based Hydrological Model (TOPMODEL), as well as for environmental verification (Fick and Hijmans, 2017).

Interpolation methods employ information from site-specific weather networks, atmospheric reanalysis products, weather radar (and associated data), satellite data, or a combination of these sources to develop global or local gridded rainfall datasets. Each of these methods has its shortcomings, many of which are particularly pronounced in precipitation estimation. For instance, while weather radar offers high temporal and spatial resolution, it often has limited spatial coverage (Beck et al. 2017a). Additionally, challenges arise in regions with complex topography, where capturing high spatial-temporal heterogeneity can be difficult for some sources used to create precipitation grids, including satellite, reanalysis, atmospheric modeling, or statistical downscaling techniques (Beck et al. 2017a; Chen et al. 2014; Herold et al. 2016; Zambrano et al. 2017). Several studies have highlighted the limitations of these datasets (Sun et al. 2018; Nastos et al. 2016; Beck et al. 2017b; Camera et al. 2017; Liu et al. 2017; Hu et al. 2018; Timmermans et al. 2019). As technology and methodologies continue to develop, integrating machine learning techniques with crowd-sourced data may be key to enhancing both the data quality and usability for various climate applications (Sun et al. 2018).

The impact of climate change on rainfall presents a multi-dimensional challenge, characterized by interactions among various climatic factors and communities. Analyzing both temporal and spatial rainfall patterns emerges as a crucial research area, providing valuable insights into the complex dynamics of climate variability and change. Therefore, the precipitation patterns in Arizona State, USA, will be examined over five-year intervals since 1961 to evaluate the impact of Earth's climate system on this area and to explore significant variations over time and across geographical regions using high-resolution satel-

lite images. Additionally, precipitation patterns for each decade will be investigated to assess the effects of climate change during the period from 1961 to 2022.

1 Study area

Arizona, located in the southwestern United States, ranks 14th in population and sixth in land area. Its capital, Phoenix, is also its largest city. The state shares borders with Utah, Colorado, and New Mexico, and neighbors Nevada, California, Sonora, and Baja California. The northern regions experience heavy snow in winter and mild summers, contributing to Arizona's reputation as a major economic hub in the Sun Belt, particularly due to migration in the 1950s. Suburban growth around Phoenix and Tucson has flourished, supported by esteemed institutions like the University of Arizona and Arizona State University (All about Arizona, 2023).

Southern Arizona is renowned for its arid Basin and Range region, which supports a diverse array of xerophyte species, including cactus. This region was shaped by ancient volcanic activity, followed by cooling and subsidence. Here, summers are extremely hot, while winters remain temperate. The state's notable geographical features include Mesas, the Colorado Plateau, and various mountain ranges, similar to many other states in the Southwestern region. Although Arizona has a predominantly dry climate, it is home to the largest population of ponderosa pine trees in the world, with forests of pine constituting about 27% of the state's forest areas. The Colorado River, characterized by its numerous branching tributaries, flows through the state, shaped by the powerful erosion of sediments caused by its waters (Urban and Community Forestry Division. Arizona State Forestry Division, 2023).

The climate of Arizona is predominantly desert-like, characterized by mild winters and exceptionally scorching summers. Late fall through early spring sees minimum temperatures hovering around 16 degrees Celsius. The coldest months, from November through February, experience average temperatures ranging from 4 degrees to 24 degrees Celsius, with occasional dips below freezing. The weather begins to warm by mid-February, ushering in sunny days and refreshing gusts. From June through September, oppressive temperatures between 32 degrees and 49 degrees Celsius are typical, with desert regions occasionally reaching 52 degrees Celsius. In arid regions at elevations

around 760 meters, diurnal temperature fluctuations can peak at 46°C during the summer months. Urban areas in the state have recorded higher nighttime lows due to local warming effects.

Arizona experiences two distinct rainy seasons: Winter rains brought by Pacific cold fronts and summer rains during the monsoon season. The latter begins at the end of summer and is characterized by a sudden increase in humidity and dewpoint levels. In Phoenix, dewpoints can reach up to 27 degrees Celsius during the monsoon, leading to dangerous flash floods triggered by lightning, thunderstorms, strong winds, and sudden downpours. In response to these dangers, the Stupid Motorist Law was passed by the Arizona legislature to penalize drivers who risk their lives by attempting to cross flooded streams. While Arizona rarely encounters severe weather events like tornadoes or hurricanes, the northern part of the state, characterized by significantly higher altitudes, enjoys cooler temperatures, with colder winters and milder summers. Occasionally, Phoenix has more days above 38 degrees Celsius than any other city in the contiguous 48 states, while Flagstaff has more days below freezing (Arizona Climate. Desert Research Institute, Western Regional Climate Center, Reno, Nevada, 2023).

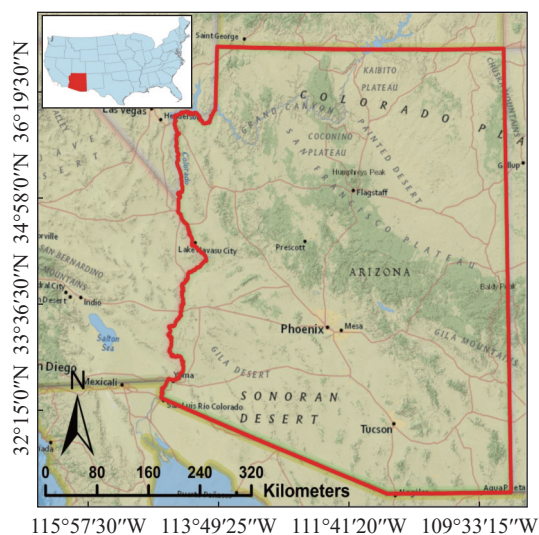


Fig. 1 Arizona State region of interest

2 CRU downloaded data

The Climatic Research Unit (CRU) has been used to download the climate data for the study area, playing a significant role in developing statistical software packages and climate models extensively used in the field. Additionally, CRU has con-

<http://gwse.iheg.org.cn>

tributed to the creation of global temperature records used for monitoring the climate system (Shi et al. 2017).

Founded in 1972 within the University's School of Environmental Sciences, the establishment of CRU was greatly influenced by the pivotal contributions of key individuals. These include Sir Graham Sutton, a former Director-General of the Meteorological Office, Lord Solly Zuckerman, who served as an advisor to the University, and Professors Keith Clayton and Brian Funnell. Notably, Professors Clayton and Funnell held the positions of Deans of the School of Environmental Sciences in 1971 and 1972. At its inception, CRU set four long-term goals (Harris et al. 2020):

1. Enhance the understanding of historical climate patterns, both recent and ancient.
2. Conduct global-scale monitoring and reporting of contemporary climatic developments.
3. Investigate the underlying processes responsible for climatic fluctuations, whether natural or human-induced, and discerning their characteristic timescales.
4. Research the feasibility of issuing advisory statements on future weather and climate trends, spanning from seasonal to multi-year horizons, grounded in scientifically accepted methods and presented in a manner beneficial for long-term planning purposes.

CRU produces multiple climate datasets, including global and regional measurements of temperature, precipitation, pressure, and atmospheric circulation. One of its most notable achievements is the CRUTEM global dataset, which tracks anomalies in land near-surface temperatures in a 5° by 5° grid-box format. The Hadley Centre for Climate Prediction and Research supplies the sea-surface temperature dataset essential for constructing the HadCRUT temperature record. Consequently, these two organizations collaborate closely in compiling this dataset.

This database, first created in the 1980s, meticulously tracks global temperature fluctuations starting from the 1850s. The terrestrial component of this record was compiled by the CRU, while the oceanic component was provided by the Hadley Centre. The IPCC relies heavily on this consolidated dataset as a primary resource for all its reports and assessments. Furthermore, CRU offers the CRU TS high-resolution gridded land surface dataset, encompassing a diverse array of environmental parameters.

While CRU primarily focuses on European climate patterns spanning the last two centuries, its research also extends to the study of Eurasian

climate over the past 10,000 years. This investigation draws upon tree-ring data and temperature records to investigate historical climate patterns in the Eurasian region during the same timeframe (Osborn and Jones, 2014).

With a grid resolution of 0.5° latitude by 0.5° longitude, CRU TS (Climatic Research Unit gridded Time Series) is a widely used climate dataset that encompasses all land areas on Earth except Antarctica. This dataset was created by interpolating monthly climatic anomalies from extensive networks of weather station observations. CRU TS was first introduced in 2000, employing Angular Distance Weighting (ADW) to interpolate monthly observation anomalies into a 0.5° grid covering global land areas). The initial dataset comprised six variables; however, subsequent update in 2004 and 2005, along with annual updates from 2006 to the present, have expanded this number to ten.

Since its inception in 2000, CRU TS has gained wide acceptance in various fields of study and practical applications. Its users come from diverse disciplines, ranging from local modeling that is weather and climate dependent (such as river catchment and agronomic studies) to global and regional climate model and reanalysis bias correction to the calibration of paleoclimate reconstructions. CRU TS is also used in fields beyond climate research, including as civil engineering, banking, and insurance (Osborn et al. 2019).

Meteorological datasets are important for estimating precipitation over large areas, particularly in regions like Arizona, where ground observations may be limited or absent. Consequently, these datasets are spatially driven by a variety of factors and includes inputs from ground-level weather stations, satellite observations, and climate model outputs. Providers of high-resolution rainfall data have made the downloaded datasets suitable for analyzing and deducing the hydrological status of the study area, allowing for the identification of environmental phenomena influenced by varying weather conditions throughout the study period. These data can be analyzed with high accuracy through interpolation techniques such as Kriging or Inverse Distance Weighting, which considers the differences between observation sites and provides a detailed understanding of rainfall distribution across different scales.

In the current research, rainfall data for the State of Arizona will be downloaded for the period from 1961 to 2022. This data will be analyzed annually to assess the extent of both negative and positive climate changes on precipitation rates, with the years 2021 and 2022 merged together for analysis.

3 Methodology

3.1 GIS processing of CRU data

To derive the annual fall rates, it is necessary to process the extensive and complex datasets downloaded for the study area, which spans a lengthy time period and covers a large portion of Arizona. The following procedures will be employed with the assistance of GIS Software.

3.2 Make NetCDF raster layer

NetCDF (Network Common Data Form) comprises a set of software libraries and data formats that are self-describing and compatible across various computing systems. These programs facilitate the creation, retrieval, and sharing of array-structured scientific data. NetCDF is particularly effective for tracking data with multiple dimensions, such as temporal and geographical variations. It integrates data and metadata into a single file, enhancing accessibility and comprehensibility for users. This format is also advantageous for applications requiring access to massive datasets. The downloaded data will be converted into NetCDF raster format using GIS applications (Morice et al. 2021) as shown in Fig. 2.

3.3 Data projection

Spatial data, whether in the form of points, lines, polygons, rasters, or annotations, is always created in a coordinate system. Coordinates can be represented in various units, including feet, meters, kilometers, or decimal degrees. The first step in selecting a suitable coordinate system is to determine the underlying measurement system accurately. The coordinate system and the data are then projected onto a flat surface, such as a piece of paper or a digital screen. This involves converting the coordinate system used on Earth's curving surface into a flat-surface equivalent through mathematical calculations. For this study, the WGS 1984 UTM Zone 12N coordinate system, which encompasses the entire state of Arizona, will be utilized.

3.4 Composite bands

The Climatic Research Unit's (CRU) reports rainfall data in Arizona on a monthly basis, and the downloaded data is organized by decade. For example, for the decade 1970–1979, 120 monthly rainfall rates (equivalent to 120 raster images)

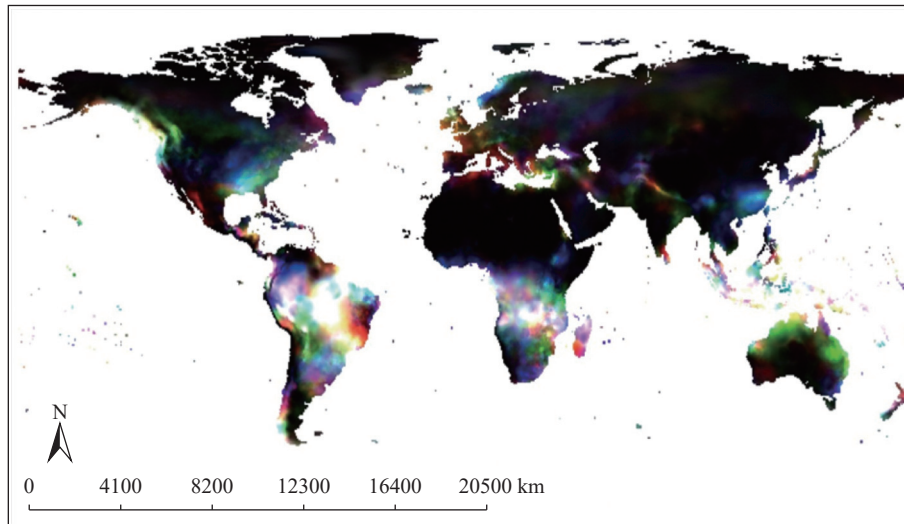


Fig. 2 Extracted CRU Data as NetCDF raster format

were downloaded, with the same number of images for the subsequent decades (1980–2020), in addition to 24 precipitation rates covering the years 2021 and 2022. In this study, precipitation data will be analyzed in five-year intervals, starting in 1970 and continuing through 2020. This means that 60 raster images will be combined for each five-year period, with 24 images combined for 2021–2022.

Raster datasets can consist of a single band, representing one characteristic, or multiple bands. A band can be seen as a matrix of cell values, and in a multi-band raster, several matrices of cell values correspond to the same geographical area. Each cell in these bands holds more than one value, which can represent different parts of the electromagnetic spectrum detected by sensors. The electromagnetic spectrum includes not only the visible range but also extends into infrared and ultraviolet regions, often used in satellite images.

When creating map layers from raster images, individual data bands can be combined into a composite band, such as in RGB (Red, Green, and Blue) color space. This process allows for displaying multiple bands together, making it easier to extract and visualize important information from the dataset. Using RGB composites provides more detailed insights compared to single-band analysis, as it leverages different parts of the spectrum for a more comprehensive view of the rainfall data (Esri ArcGIS Desktop Documentation, 2023).

3.5 Cell statistics and map algebra

This spatial analysis function computes a statistic for each cell within an output raster based on the values of corresponding cells across multiple input

rasters. For statistic types like Maximum, Minimum, Mean, Median, Majority, Minority, Percentile, and Sum, when a single raster is utilized as the input (as in this research, where each decade uses a composite band), the resulting cell values will match those in the input raster.

Map Algebra is a versatile and powerful algebraic framework used to perform all Spatial Analyst tools, operators, and functions for geographical analyses. It serves as a mathematical framework for manipulating geographic data, primarily in the form of fields. Map Algebra allows for the generation of a new raster layer (map) from one or more raster layers (maps) of the same dimensions, by applying mathematical or other specified operations (Jensen, 2016).

In this research, since composite bands are applied to monthly rainfall data for every five years, cell statistics will be utilized to calculate the total rainfall intensity for each five-year interval. The annual average rainfall intensity for each five-year period will then be derived by dividing the combined value (Resulted Raster Image) obtained from the cell statistics application by 5.

3.6 Raster to point

During this phase, the raster dataset depicting the average annual precipitation over five-year intervals, as generated through the Map Algebra step, will be transformed into point features. For each cell in the raster dataset, a corresponding point will be generated in the output feature class, representing the center of the respective cell. The conversion will exclude cells with No-Data values, ensuring that only cells with valid data are transformed into points.

3.7 Interpolation methodology (Kriging Method)

Kriging is one of several techniques used to estimate a variable's value over a continuous spatial domain when only a subset of data points is available. This approach is particularly useful when estimating values like average monthly ozone levels in a city or the distribution of healthy food options across diverse areas. Kriging differs from simpler methods such as Inverse Distance Weighted Interpolation, Linear Regression, and Gaussian decays because it uses the spatial correlations between the data points to perform the interpolation process across the entire spatial domain. Unlike other methods that rely on fixed models of spatial distribution, Kriging bases its estimates on the actual spatial arrangement of the observed data points. Additionally, for each interpolated value, Kriging also provides an assessment of its associated uncertainty (Burrough et al. 2015).

Kriging assigns more weight to points that are closer to the target location and less weight to distant points during interpolation. In addition, clusters of data points are given reduced weight compared to individual, well-distributed points because their spatial arrangement is factored into the calculation. This method helps minimize the risk of inaccurate predictions. The Kriging predictor is highly regarded as an accurate interpolator because of its optimal linear prediction characteristics. It meticulously calculates the prediction error for each interpolated value, ensuring that the values produced are Best Linear Unbiased Predictors (BLUPs). This accuracy ensures that the Kriging-generated values at each sampled location perfectly match the observed values at those points. Although Kriging may not outperform simpler interpolation techniques when there is minimal spatial autocorrelation among the sampled data points, it excels in situations where there is any degree of spatial autocorrelation. In such case, Kriging preserves spatial variability that could be overlooked when using more straightforward methods.

The Kriging process begins by fitting a variogram to the data, which reveals the spatial covariance structure among the data points. The derived covariance structure is then utilized to assign weights that interpolate values for unobserved points across the spatial domain (Krige, 1951). A variogram, or semivariogram, is a key tool in this process, representing the covariance relationship between data point pairs. It plots the gamma value,

often referred to as "semivariance," which quantifies half the mean-squared difference between any two points against the distance, termed "lag", between them. Various models, including linear, spherical, exponential, and power functions, can be used to describe the variogram depending on the dataset's characteristics (Koziel, 2011).

In Kriging, the algorithm assigns weights to each interpolated point based on the spatial proximity of the sampled points. These weights reflect the spatial structure of the data, which is captured through the variogram. Once the weights are calculated, the following formula is applied to derive the interpolated values at the target locations (Cressie, 2015):

$$\hat{Z}(X_0) = \sum_{i=1}^N \lambda_i Z(X_i) \quad (1)$$

Here, the predicted value of the target point (denoted as \hat{z} at location x_0) is obtained by summing the value of each sampled point (z at location i) multiplied by its individual weight (λ_i , specific to location i).

4 Results and analysis

This section presents the precipitation climatology patterns for Arizona State from 1961 to 2022, based on the gridded datasets. Arizona's precipitation patterns are deeply influenced by its physical geography, such as mountains, valleys, and slopes.

Orographic lifting, where moist air is pushed upward over mountain ranges, often leads to increased rainfall on the windward side of the mountains and a notable decrease, or rain shadows on the leeward side.

Rainfall distribution varies with latitude, and while Arizona is not in the equatorial region, general global trends show that equatorial regions generally receive more consistent and intense rainfall due to the convergence of trade winds. Areas near oceans, seas, or large lakes tend to have more uniform and intense rainfall. Rainfall patterns vary greatly between the dry, tropical, and temperate zones. Tropical climates are characterized by plentiful and unpredictable rainfall, while arid regions, such as much of Arizona, experience minimal water supply throughout the year.

Rainfall intensity can fluctuate due to the passage of meteorological systems such as cyclones, fronts, and monsoons. These systems play a crucial role in determining rainfall distribution and duration, as they can significantly alter atmospheric pressure and moisture content. Overall, precipita-

tion patterns can be highly diverse and complex, influenced by a combination of geographical, meteorological, and climatic factors.

Figs. 3-9 illustrate the spatial distribution of rainfall intensity across the state of Arizona for the period from 1961 to 2022, presented as annual rates for every five years. The results for the years 2021 and 2022 are combined, reflecting the annual average for these two years, in addition to the rainfall rates for each decade from 1960–2020. From Fig. 3, it is observed that rainfall rates for the first

five years of the 1960s ranged between 50–582 mm. The highest values, between 365 mm and 582 mm, were concentrated in the central regions of Arizona, while the far eastern and western areas experienced significantly lower annual rainfall rates. By the last five years of the 1960s, rainfall rates decreased in both the western and eastern regions of the state, while the central areas maintained rainfall rates ranging from 358 mm to 554 mm. Overall, the annual average for the 1960s fluctuated between 51 mm and 568 mm, which are

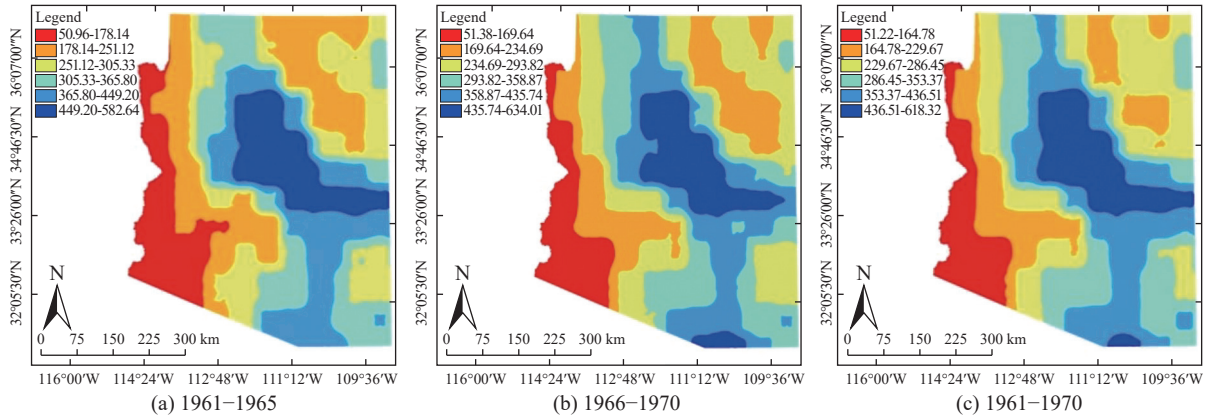


Fig. 3 Spatial distribution of the annual precipitation rates over the period from 1961–1970

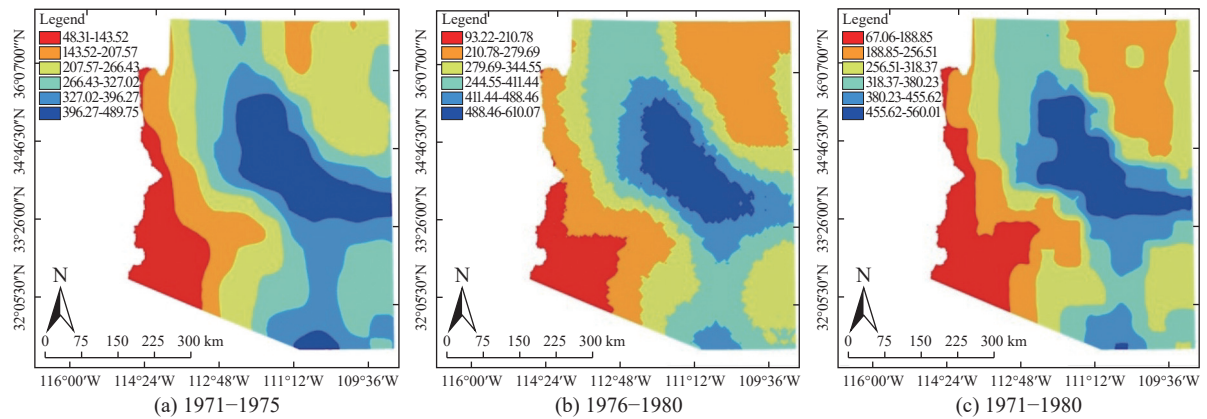


Fig. 4 Spatial distribution of the annual precipitation rates over the period from 1971–1980

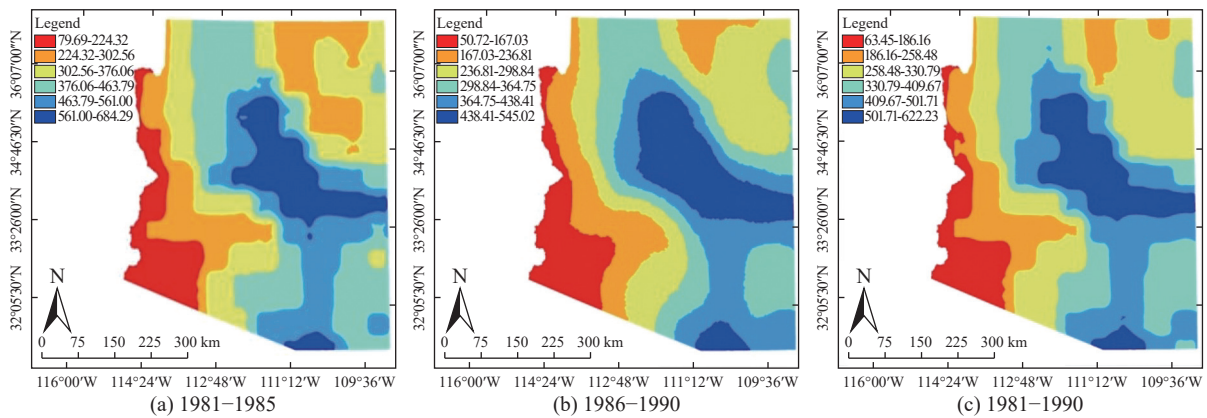


Fig. 5 Spatial distribution of the annual precipitation rates over the period from 1981–1990

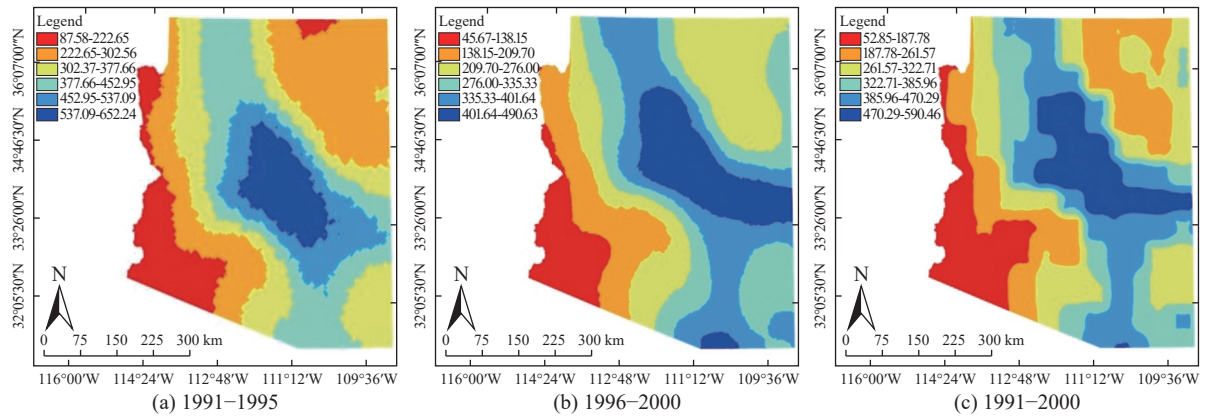


Fig. 6 Spatial distribution of the annual precipitation rates over the period from 1991–2000

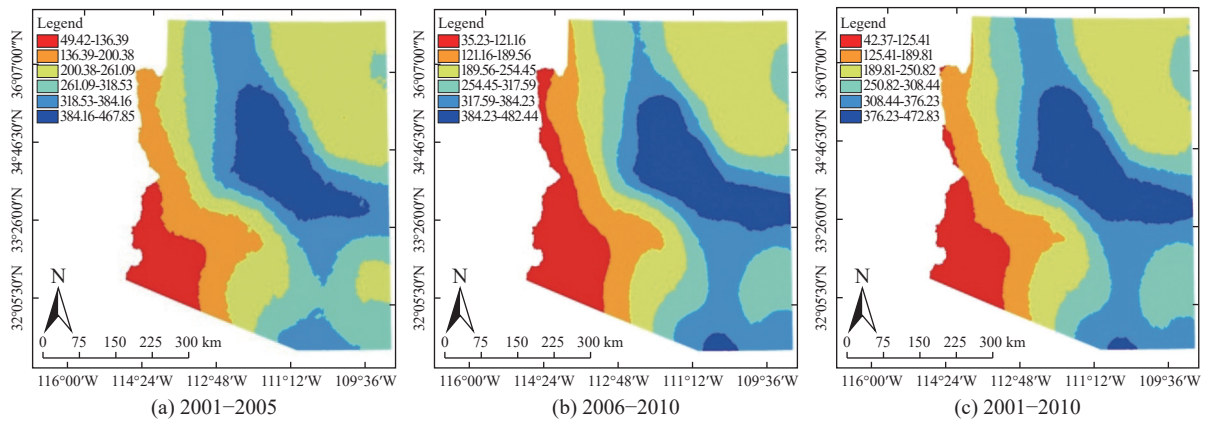


Fig. 7 Spatial distribution of the annual precipitation rates over the period from 2001–2010

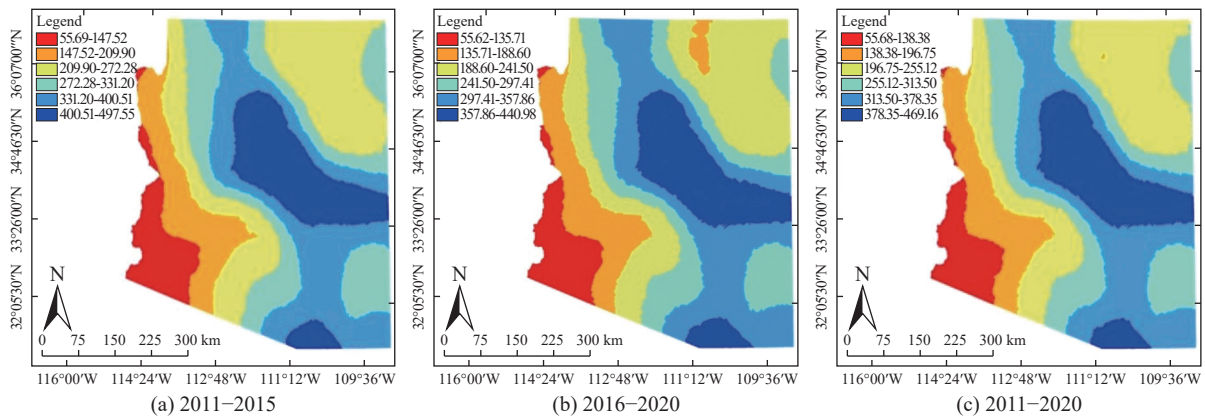


Fig. 8 Spatial distribution of the annual precipitation rates over the period from 2011–2020

considered good rates despite the intense heat experienced in the region.

In the 1970s, annual rainfall rates increased, with values ranging from 67 mm to 560 mm. In the first half of the decade, rates reached a peak of 489 mm, and this trend continued in the latter half, where rainfall rates ranged from 93 mm to 610 mm. Notably, the 1970s saw increases in annual rainfall across the eastern, western, northern, and southern regions of Arizona, while the central region experienced a noticeable decrease in some

areas, as depicted in Fig. 4.

The upward trend in annual rainfall rates continued into 1980s, with decade recording rates from 63–622 mm. The first half of this decade saw rates between 79–684 mm, while the latter half ranged between 50–545 mm. During this period, central regions that had previously experienced high rainfall rates witnessed an increase, whereas areas in the far east, west, north and south observed a decline. This pattern is evident in Fig. 5.

In the first five years of the 1990s, rainfall rates

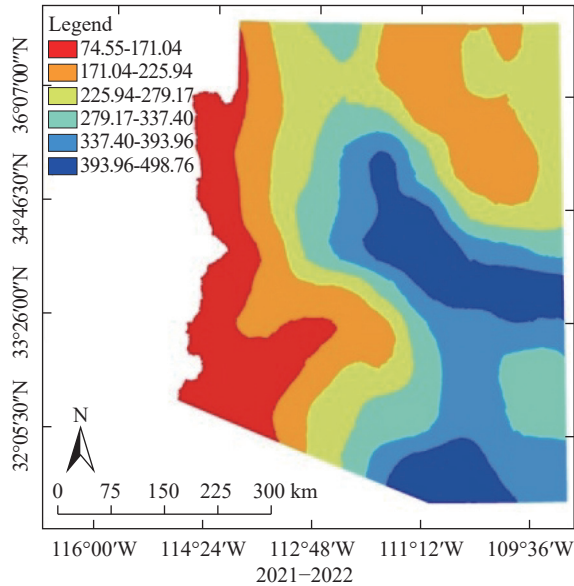


Fig. 9 Spatial distribution of the annual precipitation rates over the period from 2021–2022

in the study area continued to increase at a pace consistent with the preceding decades, ranging from 87 mm to 652 mm. However, there was a significant decline in the latter half of the 1990s, with rates dropping to between 45 mm and 490 mm, indicating a concerning decrease, given that the decline was significant and not gradual. In the initial half of the 1990s, there was a notable surge in rainfall, followed by a marked downturn in intensity during the latter half of the decade. Rainfall measurements ranged from 52 mm to 590 mm. The central zones of the state experienced heightened precipitation during the first five years, while the northern, southern, eastern, and western regions also encountered substantial rainfall amounts. This distribution contrasted with the central regions during the final five years of the decade.

As the analysis moved into the subsequent five-year period, this pattern reversed, indicating a shift in overall precipitation distribution within the study area since the 1990s. Most of the rainfall has been concentrated in the central regions of Arizona, leading to minimal precipitation reaching the western, eastern, northern, and southern parts of the state.

Delving into the insights offered by Fig. 7 reveals a fascinating panorama of rainfall dynamics during the early years of the first decade of the third millennium. Rainfall rates exhibited a spectrum ranging from 49 mm to 467 mm, with peaks reaching between 318 mm and 467 mm, particularly concentrated in the central expanse of Arizona. In contrast, the extremes in the eastern and western parts of the state experienced rela-

tively suppressed annual rainfall totals.

As the last 5 years of the 2000s unravelled, an engaging story emerged regarding changing trends in rainfall distribution. While the western and eastern fringes of the state saw an obvious decline in rainfall rates, the central regions experienced an increase with values ranging between 318 mm to 482 mm. This significant climatic shift, influenced by the ruthless march of global warming and climate transformations, resulted in annual averages rising between 42 mm and 472 mm during the early years of the new century, marking a stark departure from the climatic norms of previous decades.

In addition the story continues with Fig. 8, which represents an imaginative portrayal of rainfall patterns during the initial quinquennium of the 2020s, spanning from 2011 to 2020. Throughout this period, annual rainfall rates maintained a varied range of 55 mm to 497 mm. This visual representation validates earlier observations of a decline in annual rainfall rates during the latter half of the 2000s, characterized by a drop between 55 mm and 440 mm—a legend of nature's subtle indications of significant changes underway.

Such trends suggest that climate change has significantly impacted precipitation scarcity in the study area. Compared to preceding decades, the annual average rainfall for the 2011–2020 period markedly decreased, ranging from 55 mm to 469 mm. Over the entire ten year span from 2011–2019, the central region of the state (running north to south) consistently experienced higher rainfall rates, while the eastern and western regions exhibited persistently lower rainfall rates.

In Fig. 9, the annual average rainfall for Arizona in 2021 and 2022 was examined, revealing low values ranging between 74.55 mm and 498.76 mm. The impact of climate change remained dominant, influencing a decline in rainfall totals and exacerbating drought conditions that could worsen in the coming years and decades. Notably, the central areas of the state, particularly in the north, experienced complete loss of rainfall and are now suffering from drought, with rainfall rates significantly lower than those of previous years. Additionally, areas that previously received low rainfall have now expanded considerably, covering a vast majority of Arizona State.

5 Conclusions

Rainfall patterns are evolving unpredictably as temperatures rise, sea levels increase, and atmo-

spheric dynamics shift, resulting in both heightened and decreased precipitation across various regions. Rain, snow, sleet, and hail all play crucial roles in maintaining ecological balance and supporting multiple aspects of human life. Understanding the origins, effects, and potential solutions related to precipitation shortage is vital in today's changing world. The state of Arizona is experiencing a significant rise in temperatures, placing great pressure on terrestrial water sources, compounded by a scarcity of rainfall due to global warming.

The analysis of annual rainfall rates for the first and second five years of each decade, alongside the overall annual average for the decade, reveals important trends. The sixth, seventh, eighth, and ninth decade of the second millennium exhibited acceptable to high rainfall rates in Arizona, ranging from 51 mm to 568 mm, 67 mm to 560 mm, 63 mm to 622 mm, and 52 mm to 590 mm, respectively. Annual rates for these decades were also relatively high, though they occasionally fluctuated. Overall, precipitation rates generally ranged from 55 mm to 652 mm, with most rainfall concentrated in the central regions of Arizona, while the eastern or western areas suffered from significantly low rainfall.

In the first and second decades, as well as the initial two years of the third decade of the third millennium, signs of climate change began to manifest, casting a shadow over Arizona through a decline in rainfall rates compared to previous decades. Annual rainfall rates during the first decade ranged from 42 mm to 472 mm, the second decade from 55 mm to 469 mm, and the first two years of the third decade from 74 mm to 498 mm—values considerably lower than those recorded in the second millennium. The annual rates for every five years in the decades of the third millennium also displayed a downward trend, typically falling within the range of 35 mm to 498 mm.

The central areas of the state received higher rainfall rates compared to the outskirts to the east and west. It is increasingly apparent that climate changes and global warming are impacting rainfall rates in Arizona. This situation is likely to worsen in the future, necessitating investment in current rainfall management and exploration of alternative water sources.

The findings indicate a potential general decline in rainfall amounts in Arizona, exacerbated by uncontrolled climate fluctuations. This underscores the need to capitalize on existing rainfall by implementing effective storage solutions to counteract potential future water shortages, especially

in the eastern and western fringes of the state. Furthermore, local policies should be developed to facilitate studies addressing water availability and the implications of global warming to secure the population's water needs. The results of this research can serve as valuable inputs for crafting effective water policies aimed at mitigating these challenges.

References

- All about Arizona. 2023. Sheppard Software. Archived from the original on November 20: [updated 15 September, 2023; cited 15 September, 2023]. <https://en.wikipedia.org/wiki/Arizona>. 2017.
- Arizona Climate. 2023. Desert Research Institute, Western Regional Climate Center, Reno, Nevada. December 7, 2001. Archived from the original on December 22, 2011. [updated 15 September, 2023; cited 15 September, 2023]. <https://en.wikipedia.org/wiki/Arizona>.
- Beck HE, van Dijk AIJM, Levizzani V, et al. 2017a. MSWEP: 3-hourly 0.25° global gridded precipitation (1979–2015) by merging gauge, satellite, and reanalysis data. *Hydrology and Earth System Sciences*, 21(1): 589–615. DOI: [10.5194/hess-21-589-2017](https://doi.org/10.5194/hess-21-589-2017).
- Beck HE, Vergopolan N, Pan M, et al. 2017b. Global-scale evaluation of 22 precipitation datasets using gauge observations and hydrological modeling. *Hydrology and Earth System Sciences*, 21(12): 6201–6217. DOI: [10.5194/hess-21-6201-2017](https://doi.org/10.5194/hess-21-6201-2017).
- Behrangi A, Khakbaz B, AghaKouchak A. 2021. A satellite precipitation fusion framework (SPFusion) to produce high-resolution rainfall products. *Advances in Water Resources*, 148: 103869.
- Burrough PA, McDonnell RA, Lloyd ACD. 2015. *Principles of geographical information systems*. Third edition. Oxford: Oxford University Press.
- Camera C, Bruggeman A, Hadjinicolaou P, et al. 2017. Evaluation of a spatial rainfall generator for generating high resolution precipitation projections over orographically complex terrain. *Stochastic Environmental Research and Risk Assessment*, 31(3): 757–773. DOI: [10.1007/s00477-016-1239-1](https://doi.org/10.1007/s00477-016-1239-1).

- Cai WJ, Borlace S, Lengaigne M, et al. 2014. Increasing frequency of extreme El Niño events due to greenhouse warming. *Nature Climate Change*, 4: 111–116. DOI: [10.1038/nclimate2100](https://doi.org/10.1038/nclimate2100).
- Chen FR, Liu Y, Liu Q, et al. 2014. Spatial downscaling of TRMM 3B43 precipitation considering spatial heterogeneity. *International Journal of Remote Sensing*, 35(9): 3074–3093. DOI: [10.1080/01431161.2014.902550](https://doi.org/10.1080/01431161.2014.902550).
- Cressie NAC. *Statistics for Spatio-Temporal Data*. Wiley. 2015. DOI: [10.1080/09332480.2014.914769](https://doi.org/10.1080/09332480.2014.914769).
- Donat MG, Alexander LV, Yang H, et al. 2013. Updated analyses of temperature and precipitation extreme indices since the beginning of the twentieth century: The HadEX2 dataset. *Journal of Geophysical Research: Atmospheres*, 118(5): 2098–2118. DOI: [10.1002/jgrd.50150](https://doi.org/10.1002/jgrd.50150).
- Esri ArcGIS Desktop Documentation. 2023. <https://desktop.arcgis.com/en/>.
- Fick SE, Hijmans RJ. 2017. WorldClim 2: New 1-km spatial resolution climate surfaces for global land areas. *International Journal of Climatology*, 37(12): 4302–4315. DOI: [10.1002/joc.5086](https://doi.org/10.1002/joc.5086).
- Goddard L, Mason SJ, Zebiak SE, et al. 2001. Current approaches to seasonal to interannual climate predictions. *International Journal of Climatology*, 21(9): 1111–1152. DOI: [10.1002/joc.636.abs](https://doi.org/10.1002/joc.636.abs).
- Groisman PY, Knight RW, Easterling DR, et al. 2005. Trends in intense precipitation in the climate record. *Journal of Climate*, 18(9): 1326–1350. DOI: [10.1175/jcli3339.1](https://doi.org/10.1175/jcli3339.1).
- Harris I, Osborn TJ, Jones P, et al. 2020. Version 4 of the CRU TS monthly high-resolution gridded multivariate climate dataset. *Scientific Data*, 7(1): 109. DOI: [10.1038/s41597-020-0453-3](https://doi.org/10.1038/s41597-020-0453-3).
- Haylock MR, Hofstra N, Klein Tank AMG, et al. 2008. A European daily high-resolution gridded data set of surface temperature and precipitation for 1950–2006. *Journal of Geophysical Research: Atmospheres*, 113(D20): e2008jd010201. DOI: [10.1029/2008jd010201](https://doi.org/10.1029/2008jd010201).
- Herold N, Alexander LV, Donat MG, et al. 2016. How much does it rain over land? *Geophysical Research Letters*, 43(1): 341–348. DOI: [10.1002/2015gl066615](https://doi.org/10.1002/2015gl066615).
- Hu ZY, Zhou QM, Chen X, et al. 2018. Evaluation of three global gridded precipitation data sets in central Asia based on rain gauge observations. *International Journal of Climatology*, 38(9): 3475–3493. DOI: [10.1002/joc.5510](https://doi.org/10.1002/joc.5510).
- Huffman GJ, Bolvin DT, Braithwaite D, et al. 2017. Algorithm Theoretical Basis Document (ATBD) Version 4.6 for the NASA Global Precipitation Measurement (GPM) Integrated Multi-satellitE Retrievals for GPM (IMERG).
- Jensen JR. 2016. *Remote Sensing of the Environment: An Earth Resource Perspective*. Pearson.
- IPCC Fifth Assessment Report. <https://www.ipcc.ch/report/ar5/>. 2014.
- IPCC Sixth Assessment Report: <https://www.ipcc.ch/report/ar6/>. 2021.
- Koziel S. 2011. Accurate modeling of microwave devices using kriging-corrected space mapping surrogates. *International Journal of Numerical Modelling: Electronic Networks, Devices and Fields*, 25: 1–14. DOI: [10.1002/jnm.803](https://doi.org/10.1002/jnm.803).
- Krige DG. 1951. A statistical approach to some basic mine valuation problems on the Witwatersrand. *Journal of Chemistry Metals and Mining Society*, 52(6): 119–139.
- Liebmann B, Allured D. 2005. Daily precipitation grids for South America. *Bulletin of the American Meteorological Society*, 86(11): 1567–1570. DOI: [10.1175/bams-86-11-1567](https://doi.org/10.1175/bams-86-11-1567).
- Liu XM, Yang TT, Hsu K, et al. 2017. Evaluating the streamflow simulation capability of PERSIANN-CDR daily rainfall products in two river basins on the Tibetan Plateau. *Hydrology and Earth System Sciences*, 21(1): 169–181. DOI: [10.5194/hess-21-169-2017](https://doi.org/10.5194/hess-21-169-2017).
- Maurer EP, Hidalgo HG. 2008. Utility of daily vs. monthly large-scale climate data: An inter-comparison of two statistical downscaling methods. *Hydrology and Earth System Sciences*, 12(2): 551–563. DOI: [10.5194/hess-12-551-2008](https://doi.org/10.5194/hess-12-551-2008).
- Mishra V, Thapa S, Jha M. 2022. Spatio-temporal trends of precipitation over India using satellite-based high-resolution gridded datasets. *Remote Sensing of Environment*, 270: 112605. DOI: [10.1007/s13143-019-00120-1](https://doi.org/10.1007/s13143-019-00120-1).
- Morice CP, Kennedy JJ, Rayner NA, et al. 2021.

- An updated assessment of near surface temperature change from 1850: The HadCRUT5 data set. *Journal of Geophysical Research (Atmospheres)*, 126(3): e2019JD032361. DOI: [10.1029/2019JD032361](https://doi.org/10.1029/2019JD032361).
- Nastos PT, Kapsomenakis J, Philandras KM. 2016. Evaluation of the TRMM 3B43 gridded precipitation estimates over Greece. *Atmospheric Research*, 169: 497–514. DOI: [10.1016/j.atmosres.2015.08.008](https://doi.org/10.1016/j.atmosres.2015.08.008).
- Osborn TJ, Hulme M. 1997. Development of a relationship between station and grid-box rainfall frequencies for climate model evaluation. *Journal of Climate*, 10(8): 1885–1908. DOI: [10.1175/1520-0442\(1997\)0102.0.co;2](https://doi.org/10.1175/1520-0442(1997)0102.0.co;2).
- Osborn TJ, Jones PD, Lister DH, et al. 2021. Land surface air temperature variations across the globe updated to 2019: The CRUTEM5 data set. *Journal of Geophysical Research: Atmospheres*, 126(2): e2019jd032352. DOI: [10.1029/2019jd032352](https://doi.org/10.1029/2019jd032352).
- Osborn TJ, Jones PD. 2014. The CRUTEM4 land-surface air temperature data set: Construction, previous versions and dissemination via google earth. *Earth System Science Data*, 6(1): 61–68. DOI: [10.5194/essd-6-61-2014](https://doi.org/10.5194/essd-6-61-2014).
- Seneviratne SI, Neville N. 2012. Changes in climate extremes and their impacts on the natural physical environment. In *Managing the Risks of Extreme Events and Disasters to Advance Climate Change Adaptation*. Cambridge University Press. DOI: [10.1017/CBO9781139177245.006](https://doi.org/10.1017/CBO9781139177245.006).
- Shekhar MS, Karmakar S, Ghosh S. 2020. Future changes in precipitation extremes over South Asia using a multimodel ensemble of CMIP5 and CMIP6 simulations. *Journal of Climate*, 33(10): 4033–4053. DOI: [10.1088/1748-9326/abd7ad](https://doi.org/10.1088/1748-9326/abd7ad).
- Shi HY, Li TJ, Wei JH. 2017. Evaluation of the gridded CRU TS precipitation dataset with the point raingauge records over the Three-River Headwaters Region. *Journal of Hydrology*, 548: 322–332. DOI: [10.1016/j.jhydrol.2017.03.017](https://doi.org/10.1016/j.jhydrol.2017.03.017).
- Song XM, Mo YC, Xuan YQ, et al. 2021. Impacts of urbanization on precipitation patterns in the greater Beijing–Tianjin–Hebei metropolitan region in Northern China. *Environmental Research Letters*, 16(1): 014042. DOI: [1088/1748-9326/abd212](https://doi.org/10.1088/1748-9326/abd212).
- Sun QH, Miao CY, Duan QY, et al. 2018. A review of global precipitation data sets: Data sources, estimation, and intercomparisons. *Reviews of Geophysics*, 56(1): 79–107. DOI: [10.1002/2017rg000574](https://doi.org/10.1002/2017rg000574).
- Swain S, Mishra SK, Pandey A, et al. 2022. Spatiotemporal assessment of precipitation variability, seasonality, and extreme characteristics over a Himalayan catchment. *Theoretical and Applied Climatology*, 147(1): 817–833. DOI: [10.1007/s00704-021-03861-0](https://doi.org/10.1007/s00704-021-03861-0).
- Timmermans B, Wehner M, Cooley D, et al. 2019. An evaluation of the consistency of extremes in gridded precipitation data sets. *Climate Dynamics*, 52(11): 6651–6670. DOI: [10.1007/s00382-018-4537-0](https://doi.org/10.1007/s00382-018-4537-0).
- Trenberth KE, Dai AG, Rasmussen RM, et al. 2003. The changing character of precipitation. *Bulletin of the American Meteorological Society*, 84(9): 1205–1218. DOI: [10.1175/bams-84-9-1205](https://doi.org/10.1175/bams-84-9-1205).
- Trenberth KE. 1997. Short-term climate variations: Recent accomplishments and issues for future progress. *Bulletin of the American Meteorological Society*, 78(6): 1081–1096. DOI: [10.1175/1520-0477\(1997\)0782.0.co;2](https://doi.org/10.1175/1520-0477(1997)0782.0.co;2).
- Urban and Community Forestry Division. 2023. Arizona state forestry division. Archived from the original on July 14, 2014. [updated 15 September, 2023; cited 15 September, 2023]. Available on: <https://en.wikipedia.org/wiki/Arizona>.
- Yatagai A, Arakawa O, Kamiguchi K, et al. 2009. A 44-year daily gridded precipitation dataset for Asia based on a dense network of rain gauges. *Sola*, 5: 137–140. DOI: [10.2151/sola.2009-035](https://doi.org/10.2151/sola.2009-035).
- Zambrano F, Wardlow B, Tadesse T, et al. 2017. Evaluating satellite-derived long-term historical precipitation datasets for drought monitoring in Chile. *Atmospheric Research*, 186: 26–42. DOI: [10.1016/j.atmosres.2016.11.006](https://doi.org/10.1016/j.atmosres.2016.11.006).
- Zhang L, Li X, Zheng DH, et al. 2021. Merging multiple satellite-based precipitation products and gauge observations using a novel double machine learning approach. *Journal of Hydrology*, 594: 125969. DOI: [10.1016/j.jhydrol.2021.125969](https://doi.org/10.1016/j.jhydrol.2021.125969).